

An equivalent fluid representation of a layered elastic seafloor for acoustic propagation modelling

Matthew W Koessler (1)

(1) Marshall Day Acoustics, 6/448 Roberts Rd Subiaco, Australia

ABSTRACT

Modelling range dependent sound propagation over layered elastic seafloors with high shear speeds has proved to be a difficult problem for many widely used under water acoustic sound propagation models. Recent research and numerical developments have shown that it is possible to obtain accurate results for these types of range dependent environments, however these numerical methods are not as yet available for general use. This article explores the appropriateness of using an equivalent fluid approximation to represent the reflection phenomena associated with a layered elastic seafloor. The focus is on layered calcareous seafloors that are typical of the Australian continental shelf. A complex density approximation is used to best match a fluid plane-wave reflection coefficient to an elastic plane-wave reflection coefficient in order to determine the equivalent fluid bottom parameters. Synthetic signals are computed using Fourier synthesis to compare reflection from the equivalent fluid bottom and the original elastic bottom. The sound exposure level and peak pressure level, commonly used for practical purposes, are computed from these synthetic signals to assess the accuracy of the equivalent fluid approximation.

1 INTRODUCTION

In shallow water environments, acoustic signals interact strongly with the seafloor, therefore the type of seafloor sediments can have a significant effect on the sound field in the water column. Unconsolidated sediments are commonly described as a fluid material and solid rock is described as an elastic material (Hamilton, 1980, Hamilton, 1982). In Australia large portions of the continental shelf and upper slope are characterised by small amounts of unconsolidated sediments that overlay cemented and semi-cemented sedimentary layers (Bird, 1979, James and Bone, 2011). These seabeds predominantly consist of cemented calcareous material and are generally referred to as a calcarenite (Duncan et al., 2009).

Difficulties arise in modelling acoustic propagation over calcarenite seabeds in range dependent environments. Acoustic propagation models based on the Parabolic Equation method have been widely used for shallow water range dependent propagation modelling. The RAM (Range dependent Acoustic Model) family of propagation models are a robust and widely used implementation of the parabolic equation method. Two variants exist that are appropriate for layered fluid, RAMGeo (Collins, 1993b) and layered solid seabeds RAMSGeo (Collins, 1993a). However, RAMSGeo has been observed to produce unrealistic results when thin layers are present (Milinazzo et al., 1997, Duncan and McCauly, 2008). There are new PE models that are capable of modelling propagation over seafloors with thin elastic layers however they are not as of yet available for general use (Collis and M. Metzler, 2014). The aim here is to investigate the use of an equivalent fluid approximation such that it may be used with a fluid only parabolic equation algorithm, such as RAMGeo, for modelling acoustic propagation in range dependent shallow water environments with layered calcarenite seabeds.

2 THEORY

2.1 PLANE-WAVE AND EQUIVALENT FLUID REFLECTION COEFFICIENT

Considering a planar interface between two different media and an incident propagating acoustic wave, the plane-wave reflection coefficient (Jensen et al., 2011, Hovem, 2012), R is defined as,

$$R = \frac{A^+}{A^-} \quad (1)$$

which is the ratio of upward reflected waves A^+ to downward incident waves A^- .

For two different fluid media with different densities and sound speeds the reflection coefficient is defined as,

$$R(k_r) = \frac{\rho_2 \gamma_1 - \rho_1 \gamma_2}{\rho_2 \gamma_1 + \rho_1 \gamma_2} \quad (2)$$

where ρ_1 and ρ_2 are the densities in the upper and lower media respectively and γ_1 and γ_2 are the vertical wavenumbers of waves in the upper and lower media and k_r is the horizontal wavenumber. The sound speed in each medium is related to the vertical wavenumber through the wavenumber, which is given by

$$k = \frac{\omega}{c} \quad (3)$$

where ω is the angular frequency, c is the wave speed. The wavenumber k is related to γ by

$$k^2 = \gamma^2 + k_r^2. \quad (4)$$

When the lower medium is an elastic material the reflection coefficient (Brekhovskikh, 1960) can be written as,

$$R(k_r) = \frac{\rho_2 \gamma_1 P(k_r) - \rho_1 \gamma_{p,2}}{\rho_2 \gamma_1 P(k_r) + \rho_1 \gamma_{p,2}} \quad (5)$$

where the factor $P(k_r)$ is,

$$P(k_r) = \left(1 - \frac{2k_r^2}{k_s^2}\right)^2 + \frac{4\gamma_{p,2}\gamma_{s,2}k_r^2}{k_s^4} \quad (6)$$

The subscripts p and s denote quantities related to compressional and shear waves in the elastic bottom. The reflection coefficient can also be written as a function of grazing angle θ by using the following transformation,

$$R(k_r) \rightarrow R(\theta) \quad \text{where} \quad \cos(\theta) = \frac{k_1}{k_r} \quad (7)$$

here k_1 is the wavenumber in the upper medium.

These reflection coefficient formulae are valid for reflection from a fluid halfspace (Equation 2) or an elastic halfspace (Equation 5). They are not appropriate for a layered structure of either fluid and/or elastic material.

Computing the reflection coefficient in a fluid from a stack of elastic layers is generally more difficult than for a stack of fluid layers. An excellent reference that discusses the computation of a reflection coefficient from a layered elastic seabed can be found in Westwood et al. (1996). In the results section (Section 4) the reflection coefficient model BOUNCE (Porter, 2007) was used to compute the reflection coefficient from a stack of solid layers in the seabed. Since we are concerned with equivalent fluid approximations we only present a reflection coefficient formula for layered isovelocity fluid media. For a stack of fluid layers the reflection coefficient at the top of the stack can be computed using a recursive formula (Jensen et al., 2011, Hovem, 2012). For an M number layered of media, where M is the lower most halfspace, the m-1th fluid reflection coefficient (Hovem, 2012) can be written as,

$$\mathcal{R}_{m-1} = \frac{R_{m-1} + \mathcal{R}_m e^{2i\gamma_m h_m}}{1 + R_{m-1} \mathcal{R}_m e^{2i\gamma_m h_m}} \quad \text{where} \quad m = M - 1, \dots, 2, 1 \quad (8)$$

where the \mathcal{R}_{m-1} denotes the total reflection coefficient at an interface. The R_{m-1} reflection coefficient denotes the local reflection coefficient at an interface between m-1th and mth layers which can be calculated using Equation 2, γ_m is the vertical wavenumber in a layer and h_m is the layer thickness. This algorithm is commonly known as the invariant embedding method (Jensen et al., 2011, Hovem, 2012). It is implemented by moving upward from the bottom interface through each layer until the last interface. It is possible to specify a fluid-elastic reflection coefficient for the bottom interface using Equation 5.

3 DETERMINING EQUIVALENT FLUID BOTTOM PARAMETERS

There are several methods for approximating a solid seafloor as an equivalent fluid (Tindle and Zhang, 1992, Zhang and Tindle, 1995). When the shear wave speed is larger than the sound speed in water, like the case of solid basalt or granite rock (Hamilton, 1980, Hamilton, 1982), the solid reflection coefficient can be approximated by a fluid reflection coefficient where the shear wave speed of the solid is set as the acoustic wave speed of the equivalent fluid (Jensen et al., 2011). A more challenging scenario is when shear wave speed is less than the

sound speed in water. For low shear speed seabeds, the complex density equivalent fluid method has been proposed to approximate the solid reflection coefficient with a fluid reflection coefficient (Zhang and Tindle, 1995). Zhang and Tindle (1995) provide an explicit formula for this method, which involves converting the density to a complex quantity, assuming small grazing angles. The approximation begins to break down at shear speeds greater than 500 m/s. Furthermore, layers are not considered in their approximation.

A slightly different implementation of the complex density method to model the reflection from a layered calcarenite seabed is used here. The procedure to approximate a layered elastic seabed with an equivalent complex density fluid is as follows.

- Beginning with the top layer, the elastic reflection coefficient at the seafloor is computed using Equation 5 and treating the seabed as a halfspace with the acoustic properties of the top layer.
- Considering a range of trial values of complex density, the root mean square (RMS) difference between the reflection coefficient curves of the equivalent fluid and the elastic solid is computed. The parameters that yield the smallest RMS difference become the parameters of the equivalent fluid for the first layer.
- For the subsequent layers, Equation 8 is used to compute the total reflection coefficient through each equivalent layer to the next equivalent fluid elastic interface until the last interface is reached. The RMS difference is computed at each layer to identify the complex density for each layer. In this way the elastic stack is replaced with a fluid stack of layers.
- When multiple frequencies are considered the smallest RMS value over the relevant frequency range is used to determine the complex density in each layer. The algorithm then moves to the next layer.

4 Results

Table 1 shows the geoacoustic parameters that were used to test this implementation of the equivalent fluid complex density approximation. The seabed consists of a 1 metre thick layer of sandy material followed by a cemented calcarenite layer and an acoustic basement that is representative of a well-cemented sedimentary rock. The geoacoustic parameters are nominal values and are generally representative these types of rock (Duncan et al., 2009). However, in the real sea bottoms the layered structure of the seabed is likely to be much more complex than the simple test model considered here. It should be noted that there are other relatively unique seabed configurations, such as a thin cap rock layer (Duncan et al., 2013), that have not been considered here and are left for future analysis.

Table 1. Geoacoustic parameters for a test scenario

Layer	Thickness [m]	ρ [g/cm ³]	C_p [m/s]	C_s [m/s]	α_p [dB/ λ]	α_s [dB/ λ]
Thin Sand Layer – Calcarenite Bottom – Sedimentary Basement						
Water	N/A	1	1500	0.0	0.0	0.0
Thin Sand Layer	1	1.9	1700	0.0	0.7	0.0
Cemented Calcarenite	600	2.2	2600	1200	0.1	0.2
Sedimentary Basement	N/A	2.4	3200	1700	0.1	0.2

Table 2 presents the complex density values that were found for each layer over a frequency range of 2 Hertz to 100 Hertz. Figure 1 also shows the reflection coefficient obtained from the BOUNCE program compared to the equivalent fluid reflection coefficient.

Table 2. The equivalent fluid complex density parameters used for for the test scenario

Layer	ρ [g/cm ³]
Thin Sand Layer	$1.9 + 0.0i$
Cemented Calcarenite	$1.1 + 1.5i$
Sedimentary Basement	$3.0 + 1.5i$

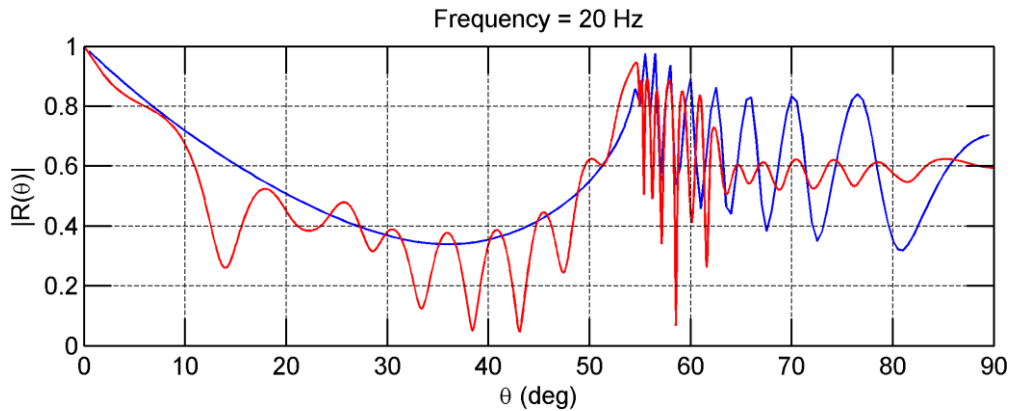


Figure 1: Comparison of the magnitudes of the reflection coefficients of the layered elastic seabed (red) and equivalent fluid seabed (blue) at a frequency of 20 Hertz.

Figure 2 shows a colour plot comparing the magnitudes of the elastic reflection coefficient and the equivalent fluid reflection coefficient over a range of frequencies from 2 Hertz to 100 Hertz.

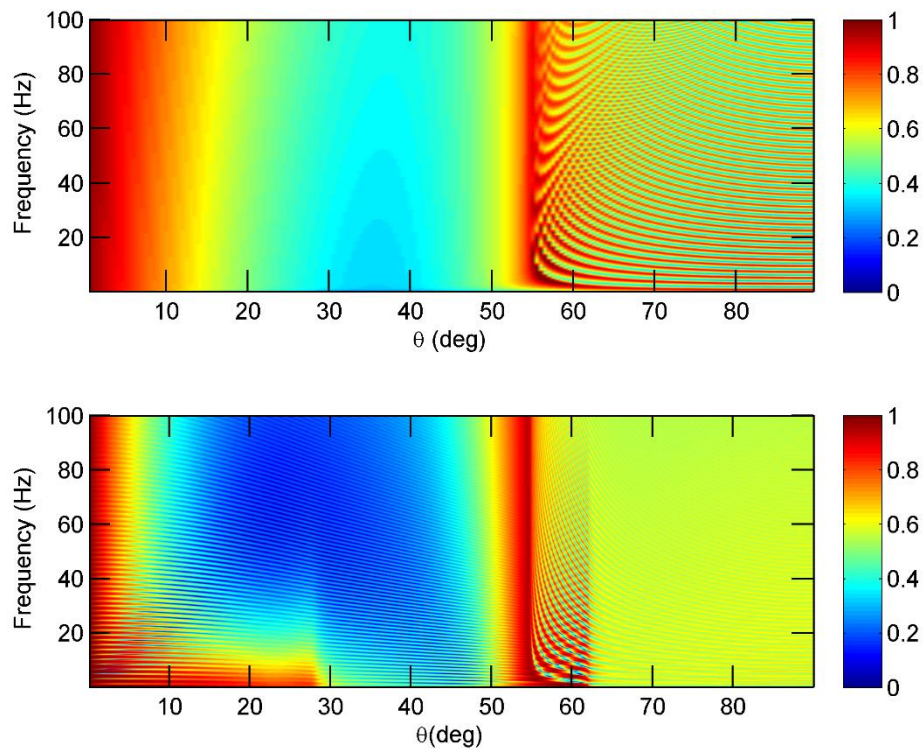


Figure 2: The magnitude of the reflection coefficient over a range of grazing angles and frequencies. *Top panel:* Magnitude of the reflection coefficient from equivalent fluid layers. *Bottom panel:* The magnitude of the reflection coefficient from elastic layers

The two reflection coefficients do not agree completely but there are features that the equivalent fluid approximates reasonably well. The critical angle is preserved in the equivalent fluid reflection coefficient and the magnitudes near critical angles are comparable between the elastic and fluid reflection coefficients. The critical grazing angle associated with the cemented calcarenite layer considered in Table 1 is 54.8°. For a calcarenite seabed the critical angle is important because a significant amount of energy can propagate in the water column as normal modes at reflected angles near the critical angle (Duncan et al., 2009). The decrease in magnitude of the two reflection coefficients up to the critical angle generally follows the same trend. However, the magnitude is larger for the equivalent fluid bottom for angles greater than the critical angle. An effect that is not reproduced in the equivalent fluid model is the frequency dependent ripples between zero degrees and the critical angle. In the

elastic reflection coefficient these are produced by shear waves that reflect off the bottom interface (Ainslie, 1995) and cannot be reproduced in an equivalent fluid approximation.

To test how well these approximations perform for practical applications, sample waveforms were compute with Fourier synthesis (Jensen et al., 2011) at different reflection angles from the elastic seabed and the equivalent fluid seabed. The incident waveform and resultant reflected waveforms are shown in Figure 3 below. The top left panel shows the incident waveform and is defined by Equation 9 below,

$$s(t) = \begin{cases} \sin(2\pi f_c(t - \tau)) - \frac{1}{2}\sin(4\pi f_c(t - \tau)), & 0 < t < \frac{1}{f_c} \\ 0, & \text{otherwise} \end{cases} \quad (9)$$

where $f_c = 20 \text{ Hz}$ and $\tau = 0.05 \text{ s}$. This incident waveform is similar to impulsive signals that are encountered in underwater acoustics.

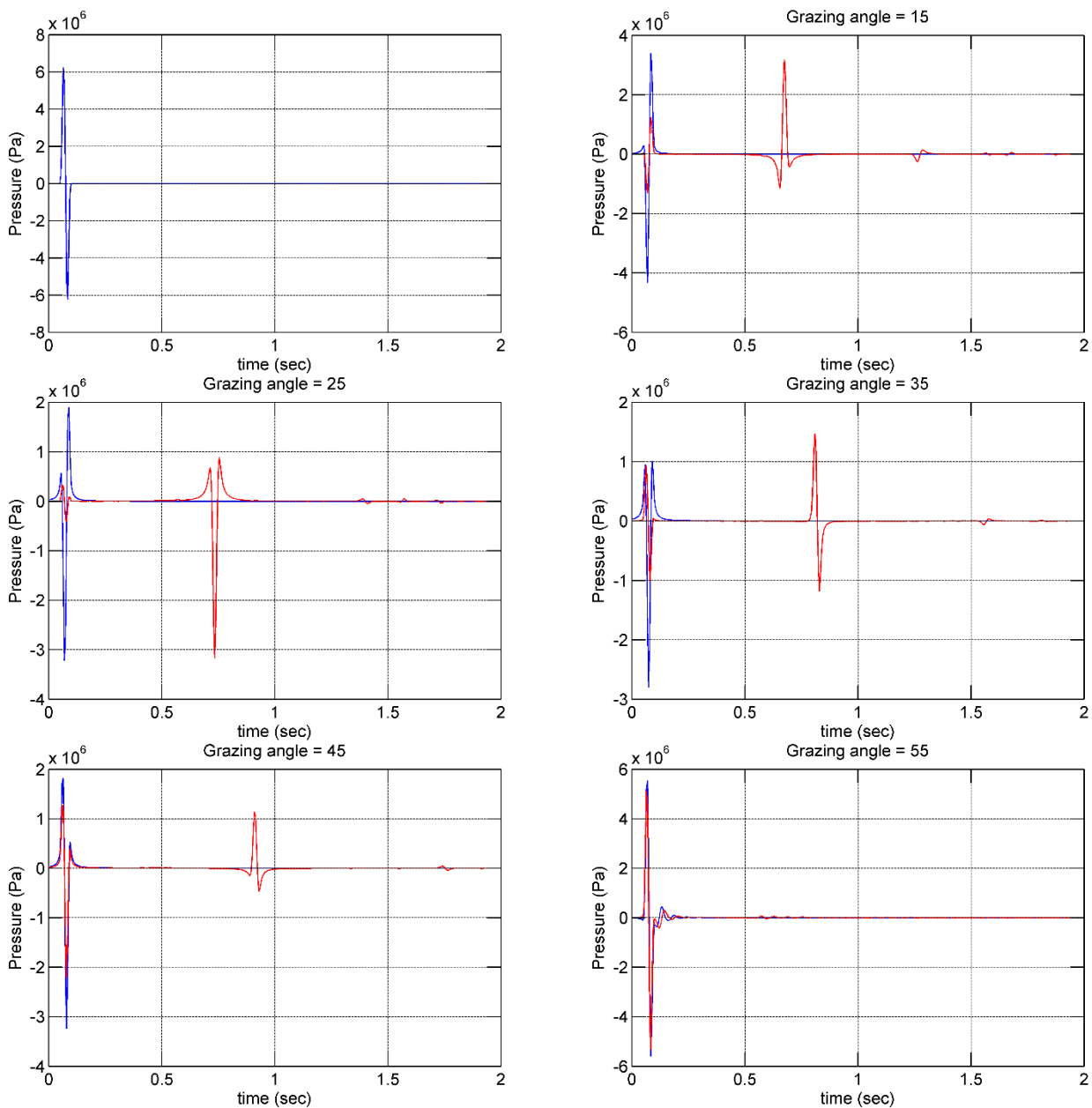


Figure 3: (Top Left Panel) Incident waveform for reflection analysis. (Other Panels): Fourier synthesized reflected waveforms from an elastic seabed (red curve) and from a complex density equivalent fluid seabed (blue curve); the grazing angle is noted on top of each panel.

The initial reflected waveforms are in reasonable agreement at grazing angles near the critical angle where these pulses have roughly the same magnitude and phase. The agreement is less robust for low grazing angles. Notably, there are multiple arrivals after the initial reflection in the signal from the elastic seabed. It is these arrivals that are associated with shear wave reflections within the elastic layers that cannot be modelled by an equivalent fluid.

From these waveforms the sound exposure level (SEL) and peak pressure level (SPL_{peak}) (Carey, 2006) were computed to assess the relative performance of the implementation complex density equivalent fluid approximation. Figure 4 shows the results over all grazing angles at 1° increments.

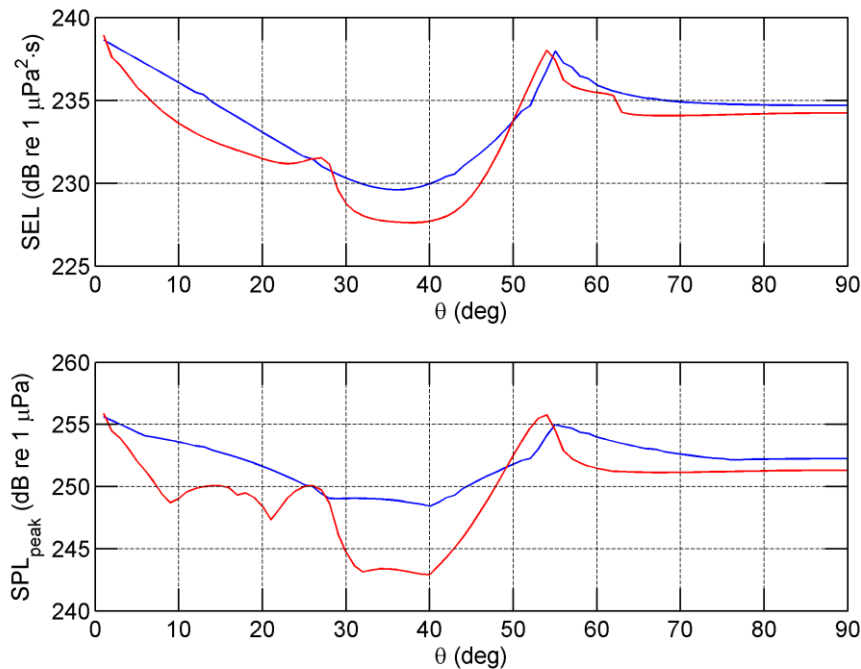


Figure 4 (*Top Panel*): Sound Exposure Level (SEL) from the reflected waveforms from an elastic seabed (red curve) and from a complex density equivalent fluid seabed (blue curve). (*Bottom Panel*): Peak pressure level (SPL_{peak}) from the reflected waveforms from an elastic seabed (red curve) and from a complex density equivalent fluid seabed (blue curve).

The major differences between the curves for the two environments, for both metrics are between the grazing angles of 15° and 50° , where the SEL and SPL_{peak} from the elastic seabed are generally lower than from the equivalent fluid seabed. The SEL which, is a measure of the energy of a signal, generally agrees better than the SPL_{peak} when comparing the two treatments of the seafloor. This comparison highlights the effect that thick elastic layers can have on reflected signals.

For grazing angles greater than the critical angle the equivalent fluid bottom will likely produce higher SEL and SPL_{peak} predictions when used with a propagation model. For grazing angles in-between zero and the critical angle there are large differences between the two reflection coefficients due to shear wave reflections, however the magnitude of the reflection coefficient is small at these angles ($|R| < 0.5$). After repeated reflections from the seafloor at these angles a signal will have lost a large portion of its initial amplitude and after several seabed interactions so the contribution of reflection to the total sound field at these angles should decrease rapidly away from the source. The confirmation of this is left to future work. In contrast, reflection near the critical angle is very important for predicting the energy of a signal propagating over a calcarenite seabed (Duncan et al., 2009, Duncan et al., 2013); particularly, because $|R| \approx 1$ which allows minimal loss upon each interaction with the seabed. Based on the results above the equivalent fluid complex density approximation might approximate propagation close to the critical angle reasonable well when used with a propagation model. Some implementations of the complex density approximation with parabolic equation models do exist (Smith, 2001, MacGillivray, 2006) but they appear to be based on the low grazing angle approximations of Zhang and Tindle (1995). An alternative approach might be to determine the complex densities in the manner discussed above then specify them as input parameters for

a propagation model through its input file. The source code of any given propagation model would have to be modified to do this.

5 CONCLUSIONS

The complex density approximation was applied to a layered elastic seabed scenario. Reasonable results were obtained by matching the reflection coefficient between an equivalent fluid seabed and elastic seabed at each layer. For calcarenite style seabeds the equivalent fluid complex density approximation preserved the amplitude and phase near the critical angle of a reflected wave when compared to the original elastic seabed. It did not correctly approximate the return of energy from shear wave reflections in the seabed at grazing angles below the critical angle. This implementation of the complex density equivalent fluid approximation may have applicability to far-field range-dependent modelling of propagation over calcarenite seabeds with parabolic equation methods.

REFERENCES

- AINSLIE, M. A. 1995. Plane-wave reflection and transmission coefficients for a three-layered elastic medium. *The Journal of the Acoustical Society of America*, 97, 954-961.
- BIRD, E. C. F. 1979. Geomorphology of the sea floor around Australia. In: PRESCOTT, J. R. V. (ed.) *Australia's Continental Shelf*. Melbourne: Thomas Nelson (Australia) in association with the Australian Institute of International Affairs
- BREKHOVSKIKH, L. M. 1960. *Waves in Layered Media*. Academic Press, New York
- CAREY, W. M. 2006. Sound sources and levels in the ocean. *Oceanic Engineering, IEEE Journal of*, 31, 61-75.
- COLLINS, M. D. 1993a. An energy-conserving parabolic equation for elastic media. *The Journal of the Acoustical Society of America*, 94, 975-982.
- COLLINS, M. D. 1993b. A split-step Pade solution for the parabolic equation method. *The Journal of the Acoustical Society of America*, 93, 1736-1742.
- COLLIS, J. M. & METZLER, A. 2014. Seismo-acoustic propagation near thin and low-shear speed ocean bottom sediments using a massive elastic interface. *The Journal of the Acoustical Society of America*, 135, 115-123.
- DUNCAN, A., GAVRILOV, A. & LI, F. Acoustic propagation over limestone seabeds. 2009. Centre for Marine Science & Technology (COE).
- DUNCAN, A. & McCauley, R. 2008. Environmental Impact Assessment of Underwater Sound: Progress and Pitfalls. *Annual Conference of the Australian Acoustical Society*. Geelong, Victoria, Australia.
- DUNCAN, A. J., GAVRILOV, A. N., MCCAULEY, R. D., PARNUM, I. M. & COLLIS, J. M. 2013. Characteristics of sound propagation in shallow water over an elastic seabed with a thin cap-rock layer. *The Journal of the Acoustical Society of America*, 134, 207-215.
- HAMILTON, E. L. 1980. Geoacoustic modeling of the sea floor. *The Journal of the Acoustical Society of America*, 68, 1313.
- HAMILTON, E. L. 1982. Sound velocity and related properties of marine sediments. *The Journal of the Acoustical Society of America*, 72, 1891.
- HOVEM, J. M. 2012. *Marine Acoustics: The Physics of Sound in Underwater Environments*, Los Altos Hills CA, Peninsula Publishing.
- JAMES, N. P. & BONE, Y. 2011. *Neritic Carbonate Sediments in a Temperate Realm*, Springer Netherlands.
- JENSEN, F. B., KUPERMAN, W. A., PORTER, M. B. & SCHMIDT, H. 2011. *Computational Ocean Acoustics*.
- MACGILLIVARY, A.O., 2006. *An acoustic modelling study of seismic airgun noise in Queen Charlotte Basin* (Masters Thesis, University of Victoria).
- MILINAZZO, F. A., ZALA, C. A. & BROOKE, G. H. 1997. Rational square-root approximations for parabolic equation algorithms. *The Journal of the Acoustical Society of America*, 101, 760-766.
- PORTER, M. B. 2007. *Acoustics Toolbox* [Online]. Available: <http://oalib.hlsresearch.com/FFP/index.html> [Accessed].
- SMITH, K.B., 2001. Convergence, stability, and variability of shallow water acoustic predictions using a split-step Fourier parabolic equation model. *Journal of Computational Acoustics*, 9(01), pp.243-285.
- TINDLE, C. & ZHANG, Z. 1992. An equivalent fluid approximation for a low shear speed ocean bottom. *The Journal of the Acoustical Society of America*, 91, 3248-3256.
- WESTWOOD, E. K., TINDLE, C. T. & CHAPMAN, N. R. 1996. A normal mode model for acousto-elastic ocean environments. *Journal of the Acoustical Society of America*, 100, 3631-3645.
- ZHANG, Z. & TINDLE, C. 1995. Improved equivalent fluid approximations for a low shear speed ocean bottom. *The Journal of the Acoustical Society of America*, 98, 3391-3396.